Ecosystems
DOI: 10.1007/s10021-009-9285-x

ECOSYSTEMS

Forest Fire Impacts on Carbon Uptake, Storage, and Emission: The Role of Burn Severity in the Eastern Cascades, Oregon

Garrett W. Meigs,[1]* Daniel C. Donato,[2] John L. Campbell,[1] Jonathan G. Martin,[1] and Beverly E. Law[1]

[1]*Department of Forest Ecosystems and Society, Oregon State University, Corvallis, Oregon 97331, USA;* [2]*USDA Forest Service, Pacific Southwest Research Station, Institute of Pacific Islands Forestry, Hilo, Hawaii 96720, USA*

Abstract

This study quantifies the short-term effects of low-, moderate-, and high-severity fire on carbon pools and fluxes in the Eastern Cascades of Oregon. We surveyed 64 forest stands across four fires that burned 41,000 ha (35%) of the Metolius Watershed in 2002 and 2003, stratifying the landscape by burn severity (overstory tree mortality), forest type (ponderosa pine [PP] and mixed-conifer [MC]), and prefire biomass. Stand-scale C combustion ranged from 13 to 35% of prefire aboveground C pools (area − weighted mean = 22%). Across the sampled landscape, total estimated pyrogenic C emissions were equivalent to 2.5% of statewide anthropogenic CO_2 emissions from fossil fuel combustion and industrial processes for the same 2-year period. From low- to moderate- to high-severity ponderosa pine stands, average tree basal area mortality was 14, 49, and 100%, with parallel patterns in mixed-conifer stands (29, 58, 96%). Despite this decline in live aboveground C, total net primary productivity (NPP) was only 40% lower in high- versus low-severity stands, suggesting strong compensatory effects of non-tree vegetation on C uptake. Dead wood respiratory losses were small relative to total NPP (range: 10–35%), reflecting decomposition lags in this seasonally arid system. Although soil C, soil respiration, and fine root NPP were conserved across severity classes, net ecosystem production (NEP) declined with increasing severity, driven by trends in aboveground NPP. The high variability of C responses across this study underscores the need to account for landscape patterns of burn severity, particularly in regions such as the Pacific Northwest, where non-stand-replacement fire represents a large proportion of annual burned area.

Key words: carbon balance; Cascade Range; disturbance; fire emissions; heterotrophic respiration; mixed-severity fire regime; net ecosystem production; net primary productivity; *Pinus ponderosa*; wildfire.

Received 22 April 2009; accepted 10 August 2009

Author Contributions: G.M. contributed to the study design, conducted field work and data analysis, and wrote the manuscript. D.D., J.C., and J.M. contributed to the study design, field work, data analysis, and writing. B.L. conceived the study, guided design and methods, and contributed to data analysis and writing.

**Corresponding author; e-mail:* gmeigs@gmail.com

Published online: 30 October 2009

Introduction

Forest ecosystems play a vital role in the global carbon (C) cycle, and spatiotemporal variability due to disturbance remains an active frontier in C research (Goward and others 2008; Running 2008).

With increasing focus on forests in the context of climate change and potential mitigation strategies for anthropogenic C emissions (Birdsey and others 2007; IPCC 2007), it is important to quantify the impacts associated with anthropogenic and natural disturbance regimes, particularly wildfire. Although numerous studies have investigated the effects of fire on C dynamics, very few to date have analyzed the full gradient of burn severity and quantified pyrogenic C emission, C pools, and postfire C balance across multiple forest types in the first few years following disturbance.

Fire's role in the terrestrial C cycle has been studied extensively in the boreal zone (for example, Amiro and others 2001; Hicke and others 2003; Kurz and others 2008) and, to a lesser extent, in temperate forests (for example, Kashian and others 2006; Gough and others 2007; Irvine and others 2007), but many uncertainties remain. Like other disturbances (insects, pathogens, large storms), fire alters the distribution of live and dead C pools and associated C fluxes through mortality and regeneration, but fire also causes direct pyrogenic C emission through combustion (Amiro and others 2001; Campbell and others 2007; Bormann and others 2008). Depending on burn severity (defined here as overstory tree mortality), C transfer to the atmosphere, and from live to dead pools, can vary substantially. In some cases the amount of C released from necromass decomposition over decades can exceed the one-time emission from combustion (Wirth and others 2002; Hicke and others 2003). One key uncertainty is the magnitude of pyrogenic C emission and the relative combustion of different C pools (Campbell and others 2007). Another important uncertainty is the rate at which postfire vegetation net primary productivity (NPP) offsets the lagged decomposition of necromass pools and their effects on net C uptake (that is, net ecosystem production [NEP]; Wirth and others 2002; Chapin and others 2006). A third uncertainty is the dynamics of heterotrophic respiration (R_h) and soil C over the first few years postfire. Although fire might increase R_h or facilitate soil C loss, recent studies in Oregon and California have shown that both can be remarkably conserved following disturbance, buffering potential negative spikes in postfire NEP (that is, C source to atmosphere; Campbell and others 2004, 2009; Irvine and others 2007). A final uncertainty is the distribution and abundance of understory vegetation—shrubs, herbs, and regenerating trees—which influence both short-term NPP trends and C balance through succession. All of these ecosystem responses and uncertainties might diverge radically in high- versus low-severity stands, but most fire-carbon studies have been limited to stand-replacement events. For example, regional and continental C models typically ignore low-severity fire, largely due to remote-sensing detection limitations and assumed minor C impacts (Turner and others 2007), despite the inherent heterogeneity of fire effects across forest landscapes.

The area burned by wildfire has increased in recent decades across western North America due to an interaction of time since previous fire, forest management, and climate (Westerling and others 2006; Keane and others 2008). Recent fires have also exhibited increasing severity, but low- and moderate-severity fire effects remain an important component of nearly all large wildfires (Schwind 2008; Miller and others 2009). The mixed-severity fire regime, defined by a wide range and high variability of fire frequencies and effects (that is, high pyrodiversity; Martin and Sapsis 1991), is characteristic of many forest types (Schoennagel and others 2004; Lentile and others 2005; Hessburg and others 2007) and may represent a new fire regime in other types that historically burned with lower severity (Monsanto and Agee 2008). The widespread increase in burned area, combined with the intrinsic variability of mixed-severity fire regimes, represents a potentially dramatic and unpredictable shift in terrestrial C cycle processes. In addition, historically uncharacteristic fires in some systems, including ponderosa pine (*Pinus ponderosa* Douglas ex P. Lawson & C. Lawson) forests, can push vegetation into fundamentally different successional pathways and disturbance feedbacks (Savage and Mast 2005), which may lead to long-term reductions in terrestrial C storage (Dore and others 2008).

Since 2002, wildfires have burned approximately 65,000 ha in and around the Metolius River Watershed in the Eastern Cascades of Oregon (Figure 1). These fires generated a complex burn severity mosaic across multiple forest types and a wide range of prefire conditions. The extent and variability of these fires, coupled with robust existing datasets on C dynamics in unburned forests in the Metolius area (for example, Law and others 2001a, 2003), presented a unique opportunity to investigate wildfire impacts on the terrestrial C cycle. In this study, we measured forest ecosystem responses across four levels of burn severity and two forest types 4–5 years following fire. Our research objective was to quantify the effects of burn severity on:

1. Pyrogenic carbon emission (combustion);
2. Carbon pools (mortality, storage, and vegetation response);

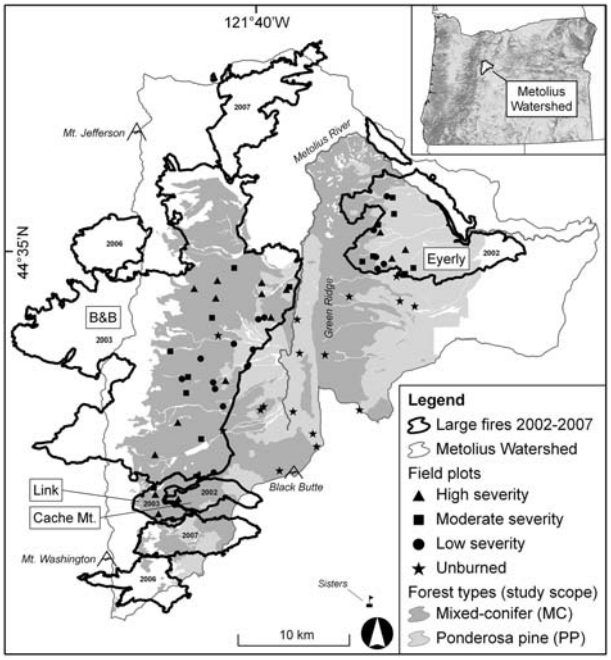

Figure 1. Metolius fire study area on the east slope of the Oregon Cascades. Point symbols denote survey plots (n = 64), labeled fires are the four surveyed (Table 2), and *shaded areas* are the sampled forest types. Other fires are outside the study scope and are labeled by fire year only. Forest type layer clipped to study scope: two types (MC and PP) on the Deschutes National Forest (DNF) within the Metolius Watershed. Other types (*unshaded area* within fires) include subalpine forests on the western margin, *Juniperus* woodlands to the east, riparian zones, and non-forest. Inset map shows study area location within Oregon elevation gradients. Fire perimeter and forest type GIS data from DNF. Other GIS data from archives at Oregon State University. Projection: UTM NAD 83.

3. Postfire carbon balance (biogenic C fluxes and NEP).

Here, we describe these three related response variables to elucidate the short-term fate of C pools and fluxes in the context of a highly heterogeneous postfire landscape.

Methods

Study Area

The Metolius Watershed is located NW of Sisters, OR, on the east slope of the Cascade Range (Figure 1). The postfire landscape is shaped by three important environmental gradients: forest type associated with climate, prefire biomass associated with past disturbance and management, and burn severity (overstory tree mortality) from recent fires.

Forest Type and Climate

The east slope is defined by one of the steepest precipitation gradients in western North America (Daly and others 2002; PRISM Group, Oregon St. Univ., http://prism.oregonstate.edu/). Within 25 km, vegetation transitions from subalpine forests (cool, wet) to *Juniperus* woodlands (warm, dry) and encompasses an unusual diversity of conifer species (Swedberg 1973). We focus on the two most prominent forest types—ponderosa pine (PP) and mixed-conifer (MC)—described by Franklin and Dyrness (1973) as the *Pinus ponderosa* and *Abies grandis* zones of Eastern Oregon. In general, the higher the elevation, mesic MC forest is more productive. Across the study area, ponderosa pine, grand fir (*Abies grandis* [Douglas ex D. Don] Lindl.), and Douglas-fir (*Pseudotsuga menziesii* [Mirb.] Franco) are the dominant tree species, and incense-cedar (*Calocedrus decurrens* [Torr.] Florin), western larch (*Larix occidentalis* Nutt.), and lodgepole pine (*Pinus contorta* Douglas ex Louden) are also abundant. Characteristic understory species include shrubs greenleaf manzanita (*Arctostaphylos patula* Greene), snowbrush (*Ceanothus velutinus* Douglas ex Hook.), and bitterbrush (*Purshia tridentata* [Pursh] DC.); forbs fireweed (*Epilobium angustifolium* L.), bracken fern (*Pteridium aquilinum* [L.] Kuhn), and American vetch (*Vicia americanum* Muhl. ex Willd.); and graminoids pinegrass (*Calamagrostis rubescens* Buckley), squirreltail grass (*Elymus elymoides* [Raf.] Swezey), and Idaho fescue (*Festuca idahoensis* Elmer). Study area elevation ranges from 600 to 2000 m, and slopes are generally gradual and east-facing. Mean annual precipitation ranges from 400 mm in eastern parts of the PP type to 2150 mm at high points in the MC type (Thornton and others 1997; DAYMET 2009). Summers are warm and dry; most precipitation falls as snow between October and June (Law and others 2001a). From W to E across the study area, average minimum January temperature ranges from −6 to −3.5°C and average maximum July temperature from 22 to 30°C (DAYMET 2009). Soils are volcanic in origin (vitricryands and vitrixerands), well-drained sandy loams/loamy sands. Additional study area characteristics are summarized in Table 1, and characteristic postfire stands are shown in Figure 2.

Historic Disturbance and Prefire Biomass

Historic fire return intervals ranged from 3 to 38 years in PP forests (Weaver 1959; Soeriaatmadhe 1966; Bork 1985; Fitzgerald 2005), from 9 to 53 years in the MC forest type (Bork 1985; Simon

Table 1. Metolius Watershed Study Area Characteristics

Forest type[1] Burn severity[2]	Number of plots	Burned area (ha) within study scope	Burned area %	Elevation (m) (mean, range)	Slope (°) (mean, range)	Total tree basal area (mean m^{-2} ha^{-1}, SE)[3]	Total tree density (mean trees ha^{-1}, SE)[3]	Tree % mortality (mean, SE)[4]
Mixed-conifer (MC)[1]	32	21,952	74	1160 (910–1558)	8.4 (1–22)	36 (3)	874 (103)	*61 (6)*
Unburned	8	na	na	1139 (910–1558)	4.9 (1–22)	35 (7)	911 (255)	13 (3)
Low severity	8	7236	25	1045 (972–1128)	6.8 (2–14)	40 (5)	1041 (252)	*29 (4)*
Moderate severity	8	4810	16	1155 (1068–1291)	10.5 (5–22)	35 (4)	1068 (142)	*58 (4)*
High severity	8	9906	33	1300 (1136–1479)	11.6 (8–14)	33 (7)	477 (81)	*96 (2)*
Ponderosa pine (PP)[1]	32	7821	26	1004 (862–1247)	5.2 (1–22)	21 (2)	643 (91)	*54 (8)*
Unburned	8	na	na	1035 (862–1247)	5.5 (1–17)	24 (4)	1020 (247)	6 (2)
Low severity	8	2371	8	977 (910–1074)	5.5 (1–22)	27 (5)	515 (122)	*14 (4)*
Moderate severity	8	2827	9	1046 (921–1092)	4.1 (1–7)	14 (3)	461 (122)	*49 (7)*
High severity	8	2623	9	957 (902–1063)	5.8 (1–15)	18 (5)	578 (168)	*100 (0)*
Overall	64	29,773	100	1082 (862–1558)	6.8 (1–22)	28 (2)	759 (70)	*58 (5)*

*Notes: Study scope was the area available for field sampling: Deschutes National Forest (DNF) non-wilderness land at least 50 m from roads, non-forest, and riparian areas. These area estimates also used for landscape scaling of pyrogenic C emission (Table 3). Note the uneven distribution of severity*type treatments across the sampled landscape.*

[1]*Determined from DNF plant association group GIS data. Forest type rows describe sum or mean values as applicable.*

[2]*Determined from DNF BARC burn severity GIS data.*

[3]*Mean basal area and density of all trees with DBH more than 1 cm, including live and dead. SE in parentheses.*

[4]*Mean% basal area mortality due to fire for burned stands (indicated by italics), mean% dead tree basal area for unburned plots. SE in parentheses.*

Figure 2. Characteristic forest stands across the Metolius Watershed study gradients. Clockwise from top-left: **A** unburned MC, **B** low-severity PP, **C** moderate-severity MC, **D** high-severity PP. Unburned stands contain heavy fuel accumulations and high tree and understory vegetation density; low-severity stands show partial bole scorching, high tree survivorship, and rapid recovery of surface litter; moderate-severity stands show increased bole scorch heights and overstory mortality; high-severity stands show near 100% tree mortality and generally thick understory vegetation (shrubs and herbs). Note that almost all fire-killed trees remain standing 4–5 years postfire.

1991), and up to 168 years in subalpine forests (Simon 1991). Given abundant lightning ignitions (Rorig and Ferguson 1999), it is likely that historic fires burned multiple forest types and exhibited the high spatiotemporal variability in fire behavior characteristic of mixed-severity fire regimes. During the twentieth century, fire suppression, grazing, timber harvest, and road construction resulted in fire exclusion. Dispersed patch clearcutting was the primary disturbance in recent decades, and most low biomass areas were young plantations (Deschutes National Forest [DNF] silvicultural GIS data). Anomalously dry, warm years (1985–1994, 2000–2005), contributed to regional drought stress (Figure 3; Thomas and others 2009). Beginning in 1986, an outbreak of western spruce budworm (*Choristoneura occidentalis*) and bark beetles (Family *Scolytidae*) killed trees across mid-to-high elevation MC forests (Franklin and others 1995). These interacting factors—time since previous fire, forest management, drought, and insect outbreaks—created fuel conditions conducive to large-scale wildfire.

Recent Large Wildfires

Since 2002, multiple large (>1000 ha) wildfires have affected half of the forested area in the watershed, burning across multiple forest types, land ownerships, and a wide range of fuel, weather, and topographic conditions. Surface, torching, and active crown fire behavior yielded a heterogeneous spatial pattern of burn severity (overstory tree mortality) at stand- and landscape-scales. This study focused on 4 major fires that burned approximately 35% of the watershed in 2002–2003 (Table 2, Figure 1).

Sampling Design and Scope

We measured postfire C pools and fluxes at 64 independent plots across the Metolius Watershed (Figure 1), sampling burned stands in 2007 (4–5 years postfire) and unburned stands in 2008. We employed a stratified random factorial sampling design with two factors—forest type and burn severity—and included prefire biomass as a covariate. We mapped forest type and burn severity

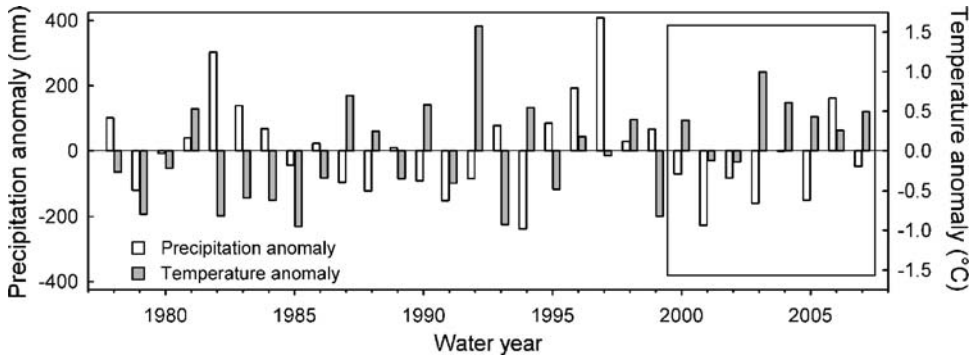

Figure 3. Climate anomalies in the Metolius Watershed. Anomalies in precipitation (mm) and temperature (°C) are in reference to the 30 year mean (1978-2007) from PRISM data (http://prism.oregonstate.edu/) extracted at a central location in the watershed (described by Thomas and others [2009]). Water year is defined as the 12-month period from October–September. The 2000 water year marked the beginning of an anomalously warm and dry period, coincident with a positive phase of the Pacific Decadal Oscillation (Thomas and others 2009). These anomalies contributed to drought stress and set the stage for wildfires and potentially harsh conifer regeneration conditions.

Table 2. Four Large Fires in the Metolius Watershed

Fire name	Fire size (ha) within watershed	Fire year	Ignition source
B&B Complex[1]	28,640	2003	Lightning
Eyerly Complex	9362	2002	Lightning
Link	1453	2003	Human
Cache Mt.	1376	2002	Lightning
Fire total	40,831		
Fire within MC and PP forest types (scope)	29,773		
Metolius Watershed area	115,869		

Note: [1]Booth and Bear Butte Complex: two large fires that merged into one.

classes from DNF GIS data. For forest type, we used a plant association group layer and combined wet and dry PP into one type and wet and dry MC into another. For burn severity, we used maps derived from the differenced normalized burn ratio (dNBR; Key and Benson 2006) classified as unburned, low, moderate, and high by DNF technicians following field assessment. Although the remotely sensed dNBR index has both known and unknown limitations (Roy and others 2006; French and others 2008), it is highly correlated with fire effects on vegetation and soil and has been used widely in conifer forests (Key and Benson 2006; Thompson and others 2007; Miller and others 2009). We defined plot-level burn severity as overstory tree basal area mortality (%), verified that plot-level mortality was consistent with the dNBR severity classes, and used the severity classes as a categorical variable (factor) in statistical analyses (described below). We used GIS to establish eight randomized survey plots within each combination of forest type and burn severity (hereafter 'type*severity treatment'; $n = 64$; Table 1, Figure 1). All plots were on DNF non-wilderness land at least 50 m from roads, non-forest, salvage-logged, and riparian areas. In addition, we used a live, aboveground biomass map from 2001 to sample the full range of prefire biomass and to ensure comparability among type*severity treatments. This biomass map was derived from regression tree analysis of Landsat spectral data and biophysical predictors (S. Powell, Univ. Montana, unpublished manuscript).

We used standard biometric methods described previously (Law and others 2001a, 2003; Campbell and others 2004; Irvine and others 2007). Below, we summarize these methods and provide specifics regarding postfire measurements, which are described in further detail by Meigs (2009). Each plot encompassed a 1 ha stand of structurally homogenous forest, which we sampled with a plot design similar to the USDA Forest Inventory and Analysis protocol (USDA 2003) enhanced for C budget measurements including tree increment, forest floor, fine and coarse woody detritus, and soil CO_2 effluxes (protocols in Law and others 2008). We scaled all measurements to slope-corrected areal units for comparison across study treatments.

Like other fire studies, this natural experiment lacked experimental control and detailed prefire data, but remotely sensed prefire biomass, GIS data, and plot attributes allowed us to account for preexisting differences. Because the forest type, burn severity, and prefire biomass were not randomly assigned, we limited statistical inference and

interpretations to the sampled forest types. To minimize potential confounding effects of spatial and temporal autocorrelation, we located plots at least 500 m apart, maximized interspersion within study area gradients, and sampled multiple fires from two different years. The experimental unit was the 1 ha plot.

Ecosystem Measurements

Aboveground C Pools, Productivity, and Heterotrophic Respiration

At each plot, we quantified aboveground C pools in four circular subplots (overstory trees, stumps, understory vegetation, forest floor) and along transects (coarse woody detritus [CWD], fine woody detritus [FWD]). We sampled overstory trees at various scales to account for different stem densities (10 m default subplot radius for trees 10.0–69.9 cm diameter at breast height [DBH; 1.37 m]). For all trees with DBH at least 1 cm, we recorded species, DBH, height, % bark and wood char, decay class (1–5; Maser and others 1979; Cline and others 1980), and whether or not trees were broken and/or dead prior to burning. We estimated CWD and FWD volume using line intercepts (Van Wagner 1968; Brown 1974; Harmon and Sexton 1996; Law and others 2008), recording diameter, decay class, and char class on four 75 m transects per plot. We sampled CWD (all pieces ≥7.62 cm diameter) along the full 300 m and FWD less than 0.64, 0.65–2.54, and 2.55–7.62 cm along 20, 60, and 120 m, respectively.

We sampled understory vegetation (tree seedlings [DBH < 1 cm], shrubs, forbs, graminoids), and ground cover in four 5 m radius subplots nested within overstory tree subplots. For tree seedlings, we recorded species, age, height, and live/dead status and identified seedlings established before fire. Based on seedling age and DNF GIS replanting data, we determined if seedlings were planted and excluded these from natural regeneration analyses. We calculated shrub volume from estimates of live shrub % cover in three height classes (0–0.5, 0.5–1.0, 1.0–2.0 m) and dead shrub stem number, length, and diameter. We estimated the % cover of forbs, graminoids, litter, woody detritus, cryptogams, rocks, and mineral soil.

We computed biomass with an allometry database of species-, ecoregion-, and decay class-specific volume equations and densities (Hudiburg 2008; Hudiburg and others 2009), adjusting tree, CWD, and FWD biomass estimates for char reduction (Donato and others 2009a), broken status, and severity-specific estimates of bark, wood, and foliage combustion after Campbell and others (2007). We used species-specific allometric equations to convert live shrub volume to mass and converted dead shrub volume to mass using the mean decay class 1 wood density of three locally abundant genera (*Acer*, *Alnus*, *Castanopsis*). We converted herbaceous cover to biomass using 0.25 m^2 clip plots of dominant species sampled across the study area. We assumed that the C content of all pools was 0.51 except for forest floor (assumed to be 0.40; Campbell and others 2007). We sampled forest floor (litter and duff) to mineral soil with 10.2 cm diameter pvc corers at 16 randomized locations per plot and oven-dried samples at 60°C for more than 72 h to determine mass.

We determined NPP and heterotrophic respiration (R_h) at the 48 burned plots. We estimated bolewood NPP from radial increment measurements of current and previous live tree biomass (Van Tuyl and others 2005; Hudiburg and others 2009), collecting increment cores at breast height from 20 representative live trees in each low- and moderate-severity plot. Although researchers typically average radial increment from the previous 5-10 y to account for climatic variability (for example, Law and others 2003), we used the last full year of radial growth (2006) to estimate bolewood NPP because we could not assume a steady state 4–5 years postfire. For live trees in high-severity stands (<0.5% of inventoried trees, n = 23 at 3 of 16 stands), we applied forest type averages of increment data from low- and moderate-severity stands. We calculated foliage NPP as the product of specific leaf mass per unit area (SLA), leaf retention time (LRT), and plot-level leaf area index (LAI). We estimated SLA and LRT from representative canopy shoots with full retention and measured LAI optically using a Sunfleck ceptometer (Decagon Devices, Inc., Pullman, WA) after Law and others (2001b) and Pierce and Running (1988). Because moderate- and high-severity fire substantially altered tree crowns through combustion and mortality, we scaled LAI measurements from low-severity plots using a regression of the positive relationship between LAI and live tree basal area ($LAI = 3.85 * [1 - e^{(-0.0311 * \text{live basal area})}]$, adj. R^2 = 0.54, n = 16; fitted using the exponential rise to maximum statistical program in SigmaPlot [Version 11.0, SPSS Science, IL]). We computed shrub wood and foliage NPP from annual radial increment and LRT (Law and Waring 1994; Hudiburg and others 2009). We assumed that herbaceous

mass equaled annual NPP and that annual mass loss was 50% (Irvine and others 2007).

We computed aboveground R_h of dead woody pools (R_{hWD}) as the product of necromass and decomposition constants from a regional CWD database (Harmon and others 2005). Because snags decay much more slowly than CWD in this seasonally moisture-limited system, we assumed that snag decomposition was 10% of CWD decomposition (Irvine and others 2007), but we used CWD decomposition rates for stumps, for which microbial decay processes are less moisture-limited (M. Harmon, Oregon St. Univ., 2009, personal communication). We estimated FWD decomposition after McIver and Ottmar (2007).

Belowground C Pools, Productivity, and Heterotrophic Soil Respiration

At the 48 burned plots, we collected soil and fine roots (FR: <2 mm diameter) at 16 randomized locations per plot using 7.3 cm diameter augers. Default sampling depth was 20 cm with one core up to 100 cm per plot. We used linear regression to scale C, N, and FR to 100 cm. We assumed that 49% (SD = 14) of soil C, 48% (SD = 17) of soil N, and 62% (SD = 20) of FR were in the top 20 cm, within the variation of the FR correction factor reported by Law and others (2003). All samples were sorted through 2 mm sieves, bench-dried, mixed by subplot, and analyzed for mass fraction of C and N (LECO CNS 2000 analyzer, Leco Corp., St. Joseph, MI), texture (hydrometer method), and pH (Oregon St. Univ. Central Analytical Laboratory). We calculated bulk density via stone displacement and separated FR and other organic matter. We combusted a representative FR subsample in a muffle furnace at 550°C for 5 h to determine organic content (74.24%), which we applied to all FR samples to estimate total organic matter. Based on published estimates of regional FR decomposition (Chen and others 2002) and mortality (Andersen and others 2008), we assumed that less than 40% of fire-killed FR remained when sampled, that far fewer were retained by 2 mm sieves, and that the vast majority of sampled FR was newly recruited postfire. We estimated that live roots were 61% of total FR mass in PP stands (Irvine and others 2007) and 87% of FR mass in MC stands (P. Schwarz, Oregon St. Univ., unpublished data). We computed FR NPP as the product of total organic FR mass and a root turnover index from rhizotron measurements in a nearby unburned PP forest (Andersen and others 2008). We estimated live and dead coarse root (CR: > 10 mm diameter) mass from the tree, snag, and stump surveys as a function of DBH (Santantonio and others 1977) and computed CR NPP from modeled current and previous live tree diameters (from increment cores). Because the median stump height was 30 cm, we applied a correction factor of 0.9 to account for bole taper to 1.37 m for stump CR estimates (adapted from D. Donato, unpublished data).

We measured soil CO_2 efflux and adjacent soil temperature at burned plots during the peak flux period (12 randomized locations; one set of manual measurements per plot in late June) using a Li-6400 infrared gas analyzer with Li-6000-9 soil chamber (Li-Cor Biosciences, Lincoln, NE) and established protocols (Law and others 1999; Campbell and Law 2005; Irvine and others 2007, 2008). We estimated annual soil respiration (R_{soil}) by matching plot measurements with concurrent, hourly, automated soil respiration measurements at a nearby unburned AmeriFlux PP tower site (Irvine and others 2008). The automated record consisted of hourly measurements spanning early May to mid November and was gap-filled using 16 cm soil temperature and 0–30 cm integrated soil moisture (see Irvine and others 2008 for model specifics). We scaled plot measurements to the annual dataset using plot-specific correction factors based on the ratio of mean soil respiration for a given plot divided by the concurrent automated rate. Correction factors ranged from 0.47 to 1.60 (range of type*severity means: 0.87–1.02). This approach sampled the spatial variability of R_{soil} within each plot to determine base rates and leveraged the long-term, intensive measurements of temperature- and moisture-driven variability. Similar automated measurements were made in 2002–2003 in a MC stand that subsequently burned in the B&B fire. A comparison of MC and PP continuous respiration datasets during the overlapping measurement period indicated near identical diel amplitudes and seasonal patterns between the two sites (data not shown). Given this similarity, we concluded that annual, plot-specific R_{soil} estimates based on the PP automated soil respiration would adequately represent the spatial and temporal variation within and among plots. We computed the heterotrophic fraction of soil respiration (R_{hsoil}) based on previous measurements at vegetation-excluded automated chambers at high-severity and unburned AmeriFlux tower sites within the study area (Irvine and others 2007).

Net Ecosystem Production

We estimated net ecosystem production (NEP: the difference between gross primary production and ecosystem respiration; Chapin and others 2006) using the mass balance approach (Law and others 2003; Campbell and others 2004; Irvine and others 2007):

$$\mathrm{NEP} = (\mathrm{NPP_A} - R_{\mathrm{hWD}}) + (\mathrm{NPP_B} - R_{\mathrm{hsoil}}) \quad (1)$$

where $\mathrm{NPP_A}$ is aboveground NPP, R_{hWD} is heterotrophic respiration of aboveground woody detritus, $\mathrm{NPP_B}$ is belowground NPP, and R_{hsoil} is heterotrophic soil surface CO_2 efflux (includes forest floor). NEP is the appropriate metric of C balance and uptake at the spatiotemporal scale of our measurements, whereas net ecosystem carbon balance (that is, net biome production) describes landscape- to regional-scale C balance and longer-term effects of fire and other fluxes (for example, erosion, leaching, timber harvest; Chapin and others 2006). Here, we assume these other fluxes to be negligible during the sampling period, and we account for combustion losses independently of NEP.

Pyrogenic C Emission from Combustion

Before-after measurement of C pools is the most certain method to measure pyrogenic C emission (Campbell and others 2007), but in this study, co-located prefire measurements were not available, and it was not possible to establish a paired plot for every burned condition across the study gradients. We estimated C loss from combustion using a standard simulation program (Consume 3.0; Prichard and others 2006), augmented with field estimates of tree consumption. Consume predicts aboveground fuel consumption, C emission, and heat release based on weather data, fuel moisture, and fuelbed inputs from the Fuel Characteristic Classification System (FCCS 2.0; Ottmar and others 2007); both models available at: www.fs.fed.us/pnw/fera/. We selected representative FCCS fuelbeds for PP and MC stands (Table 3) using GIS and modified these to develop custom fuelbeds based on field measurements at the 16 unburned plots. We simulated low-, moderate-, and high-severity fire by adjusting percent canopy consumption and fuel moisture content for woody fuels and duff (R. Ottmar, US Forest Service, 2009, personal communication). Because Consume 3.0 does not account for consumption of live tree stems and bark, we used field measurements to calculate the changes in mass and density due to charring (Donato and others 2009a). We assessed combustion at the stand-scale and scaled combustion to the sampled landscape with forest type and burn severity GIS data.

Statistical and Uncertainty Analysis

We used multiple linear regression and analysis of covariance to compare response variables across the study gradients. Because one- and two-way ANOVA (forest type and burn severity tested separately and combined) revealed a significant difference in prefire biomass between the two forest types ($P < 0.001$) but no significant prefire difference among burn severities within either forest type ($P > 0.5$), we conducted analyses separately by forest type. We derived test statistics (coefficients and standard errors) from a multiple linear regression model of the response variable as a function of prefire biomass (continuous) and burn severity (categorical) within a given forest type. Regression analysis showed no significant interactions among explanatory variables; coefficient estimates were calculated from additive models with an assumption of parallel lines among type*severity treatments. We log-transformed data when necessary to satisfy model assumptions. We accounted for multiple comparisons and reported statistical significance as the highest significant or lowest non-significant Tukey-adjusted P value ($\alpha = 0.05$) common to all groups (for example, severity classes) in a given comparison (PROC GLM lsmeans multiple comparisons; SAS 9.1, SAS Institute, Inc., Cary, NC).

We take a pragmatic view of uncertainty analysis after Irvine and others (2007). Many scaling assumptions are necessary to estimate plot-level metrics from components sampled at varying spatiotemporal scales. Further, given the wide range of sampled prefire biomass and variability across the postfire landscape, it is possible to commit Type II statistical errors when important differences exist but are confounded by additional factors. We thus focus on the trends and proportions across type*severity treatments rather than absolute magnitudes. To estimate NEP uncertainty, we used a Monte Carlo procedure with the four major fluxes described in equation (1) for each type*severity treatment (NEP uncertainty expressed as ± 1 SE after 10000 iterations based on the standard normal distribution with mean, standard deviation, and between-flux covariance in R [R Development Core Team 2009]).

Table 3. Pyrogenic C Emission (PE) from Consume 3.0 Simulations and Field Measurements of Consumption

FCCS fuelbed[1]	Forest type Burn severity[2]	Stand scale				Landscape scale	
		Total aboveground C (Mg C ha^{-1})[3]	Stand-scale PE (Mg C ha^{-1})[4]	% Consumption, aboveground C[5]	% Consumption, live tree stems[6]	Total PE (Tg C)[7]	Landscape % of total PE[7]
Grand fir–Douglas fir forest	Mixed-conifer						
(fire suppression) (SAF 213)	Unburned	132.6					
	Low severity		16.6	13	0.23	0.120	16
	Mod severity		25.3	19	0.71	0.122	16
	High severity		32.3	24	2.01	0.320	42
Pacific ponderosa pine forest	Ponderosa pine						
(fire suppression) (SAF 237)	Unburned	87.2					
	Low severity		19.7	23	0.27	0.047	6
	Mod severity		25.6	29	1.43	0.072	10
	High severity		30.2	35	2.77	0.079	10
Across sampled burn area (29,773 ha)			**25.5**[8]	**22**[8]	**1.24**[8]	**0.760**	100

Notes: [1]*Fuel Characteristic Classification System (FCCS) fuelbeds determined using GIS data and descriptions from US Forest Service FERA group: www.fs.fed.us/pnw/fera/. SAF codes are Society of American Foresters cover types (Eyre 1980).*
[2]*Severity classes derived by adjusting surface fuel moisture and canopy consumption (R. Ottmar, US Forest Service, 2009, personal communication).*
[3]*Total aboveground C from unburned stands, used for parameterizing FCCS fuelbed inputs for Consume modeling. Multiply by 2 for Mg ha^{-1} mass or by 100 for g C m^{-2}.*
[4]*Pyrogenic C emission (PE) computed from simulated biomass combustion in Consume and field measurements of bark and bole charring calculated after Donato and others (2009a) and Campbell and others (2007).*
[5]*% of unburned plot aboveground C (4th column).*
[6]*% of live tree bark and bole bark mass estimated from charring (mean, weighted by tree mass).*
[7]*Stand-scale PE scaled to the sampled landscape based on area of type*severity treatments (Table 1).*
[8]*Mean, weighted by area of type*severity treatments (Table 1).*

Results and Discussion

Pyrogenic C Emission (Combustion)

Simulated mean pyrogenic C emission (PE) was 25.5 Mg C ha^{-1} (range: 16.6–32.3 Mg C ha^{-1}) and was similar between forest types. The % consumed in PP stands was substantially higher (range: 23–35 vs. 13–24% for PP versus MC stands, respectively, Table 3). Stand-scale PE from low-severity fire was 51% and 65% of high-severity PE in MC and PP stands, respectively, indicating that the largest proportion of emissions was from combustion of surface and ground fuels. This result is consistent with Campbell and others (2007), who determined that greater than 60% of total combustion was from litter, foliage, and small downed wood, and that these high surface area:volume ratio pools were readily consumed (>50% combusted) in all burn severities in SW Oregon mixed-conifer forests. Our field-based estimate of live tree stem consumption was on average 1.24% (range: 0.23–2.77%) of live bark and bole mass, a trivial amount compared to other PE uncertainties. The largest remaining uncertainty is that the Consume 3.0 model does not account for belowground C loss due to combustion, erosion, or other fire effects, which can be substantial in some cases (Bormann and others 2008). Without detailed prefire measurements, we were unable to address this issue directly, but our soil C surveys did not show any significant C declines in high-severity stands (described below).

Scaled to the sampled landscape (approximately 30,000 ha of burned area), simulated total PE was 0.76 Tg C (Table 3). High-severity MC stands, with the largest per unit area emissions and landscape area, contributed a disproportionate amount of PE (42% of the total), whereas all PP forests combined released 26% of total PE. These proportions underscore the importance of incorporating landscape patterns of vegetation and fire effects (that is, the severity mosaic) into modeling and policy analyses. On a per unit area basis, PE from these fires was 33% higher than from the 200,000 ha Biscuit Fire (25.5 vs. 19 Mg C ha^{-1}; Campbell and others 2007). This C transfer represents a substantial pulse to the atmosphere relative to annual net C fluxes from unburned forest in the Metolius area (mean annual net C uptake at a mature PP site: 4.7 ± 0.4 Mg C ha^{-1} y^{-1}; Thomas and others 2009). Conversely, 0.76 Tg C is approximately 2.5% of Oregon statewide anthropogenic CO_2 emissions from fossil fuel combustion and industrial processes for the 2-year period 2002–2003 (30.62 Tg C equivalent; http://oregon.gov/energy/gblwrm/docs/ccigreport08web.pdf). It is important to note that the study scope burned area is less than half of the area burned in and around the Metolius Watershed since 2002 (>65,000 ha, 35,000 ha beyond this study scope) and that these were large fire years regionally. Thus, our study area represents a relatively small proportion of total wildfire PE. Although further refinements are possible, the current analysis provides a reasonable constraint for regional modeling efforts.

Carbon Pools (Mortality, Storage, and Vegetation Response)

Because large C pools (that is, live tree boles) were largely unaffected by combustion in all severities, fire-induced mortality was the most important overall C transformation, larger in magnitude than combustion. The distribution of live and dead C pools changed predictably with burn severity, dominated by the shift from live trees to dead wood mass (Table 4). Aboveground live tree and dead wood mass (g C m^{-2}) both exhibited wide ranges (live tree range: 0–9302, PP high severity to MC low severity; dead wood range: 924–6252, PP low severity to MC high severity), the latter range encompassing dead wood estimates from Washington East Cascades high-severity stands (approximately 3000; Monsanto and Agee 2008). Mean basal area mortality increased with burn severity classes, ranging from 14% in low-severity PP stands to 49% in moderate-severity and 100% in high-severity PP stands, with parallel patterns in MC stands (29, 58, 96%, respectively; Table 1, Figure 4A). Across both forest types, this mortality resulted in a significant reduction in live aboveground C in high- versus low-severity stands ($P < 0.005$), coupled with a near tripling of dead wood aboveground C (Table 4). In both forest types, forest floor mass showed the largest absolute and relative difference between burned and unburned stands (mean: 1588 and 232 g C m^{-2}, respectively), consistent with near-complete combustion of these pools. Whereas the difference between burned and unburned forest floor mass was highly significant (85% reduction; $P < 0.001$), there were no significant differences among low-, moderate-, and high-severity stands in either forest type ($P > 0.850$). Because of the decline in forest floor and high tree survival, low-severity stands exhibited lower aboveground necromass than unburned stands (Table 4).

Total aboveground C and total ecosystem C declined with increasing burn severity in both forest

Table 4. Carbon Pools of Forest Stands in the Metolius Watershed

Forest type[1] Burn severity	Aboveground					Belowground			
	Live tree mass	Non-tree live mass[2]	Dead wood mass[3]	FWD[4]	Forest floor[5]	Coarse root[6]	Fine root[7]	Soil C[8]	Ecosystem C[9]
Mixed-conifer[1]	5153 (807)	156 (12)	4080 (537)	171 (15)	610 (135)	3115 (232)	*185* (*34*)	*6556* (*348*)	***18,648*** (*1213*)
Unburned	$_{ab}$9302 (1146)	$_{ab}$140 (22)	2884 (1008)	205 (31)	$_{a}$1610 (180)	3588 (480)	na (na)	na (na)	**na** (na)
Low severity	$_{abc}$7268 (1147)	$_{a}$105 (22)	2813 (1009)	166 (31)	$_{b}$374 (180)	3162 (481)	172 (62)	5960 (611)	**20,414** (2189)
Mod severity	$_{bcd}$3071 (1140)	$_{ab}$181 (22)	4371 (1003)	162 (30)	$_{b}$289 (179)	2931 (478)	211 (61)	6434 (604)	**17,884** (2163)
High severity	$_{cd}$972 (1141)	$_{b}$200 (22)	6252 (1003)	153 (30)	$_{b}$169 (179)	2780 (478)	172 (61)	7225 (604)	**17,727** (2166)
Ponderosa pine[1]	3178 (538)	104 (9)	1898 (300)	112 (16)	531 (151)	1713 (142)	*135* (*10*)	*5903* (*195*)	***12,677*** (*648*)
Unburned	$_{w}$5110 (714)	$_{wxy}$78 (14)	$_{wx}$1517 (543)	$_{w}$179 (29)	$_{w}$1566 (219)	1842 (276)	na (na)	na (na)	**na** (na)
Low severity	$_{w}$5576 (716)	$_{wx}$67 (14)	$_{w}$924 (544)	$_{wx}$75 (29)	$_{x}$234 (219)	2131 (276)	128 (18)	6034 (353)	$_{w}$**15,244** (922)
Mod severity	$_{x}$2098 (724)	$_{xyz}$126 (14)	$_{wx}$1934 (551)	$_{wx}$130 (30)	$_{x}$258 (222)	1563 (280)	141 (18)	5899 (359)	$_{wx}$**12,089** (937)
High severity	$_{x}$0 (0)	$_{yz}$146 (14)	$_{x}$3218 (542)	$_{x}$64 (29)	$_{x}$67 (218)	1317 (275)	137 (18)	5775 (351)	$_{x}$**10,677** (918)

Notes: Values: mean C pools (g C m^{-2}). SE from ANCOVA in parentheses. Subscript letters indicate pairwise significant differences (Tukey-adjusted $P < 0.05$) between severities within each forest type. To convert values to Mg biomass ha^{-1}, divide by 50.

[1]*Forest type row: non-italics denote all stands (unburned and burned, n = 32); italics denote burned stands only (n = 24, unburned stands not surveyed [na]).*

[2]*Other live pools: shrubs, seedlings, graminoids, forbs.*

[3]*Dead wood mass: sum of snags, stumps, and CWD (dead down wood ≥ 7.63 cm diameter).*

[4]*FWD: all woody fuels less than 7.63 cm diameter.*

[5]*Forest floor: sum of litter and duff.*

[6]*Coarse roots at least 10 mm diameter (modeled from diameter of live and dead trees and stumps).*

[7]*Fine roots less than 2 mm diameter (live and dead), scaled from 20 cm depth (62% [SD = 20] of fine roots assumed in top 20 cm).*

[8]*Soil C to 100 cm depth, scaled from 20 cm depth (49% [SD = 14] of soil C assumed in top 20 cm).*

[9]*Ecosystem C: sum of all C pools. Includes dead shrubs (not included in other columns).*

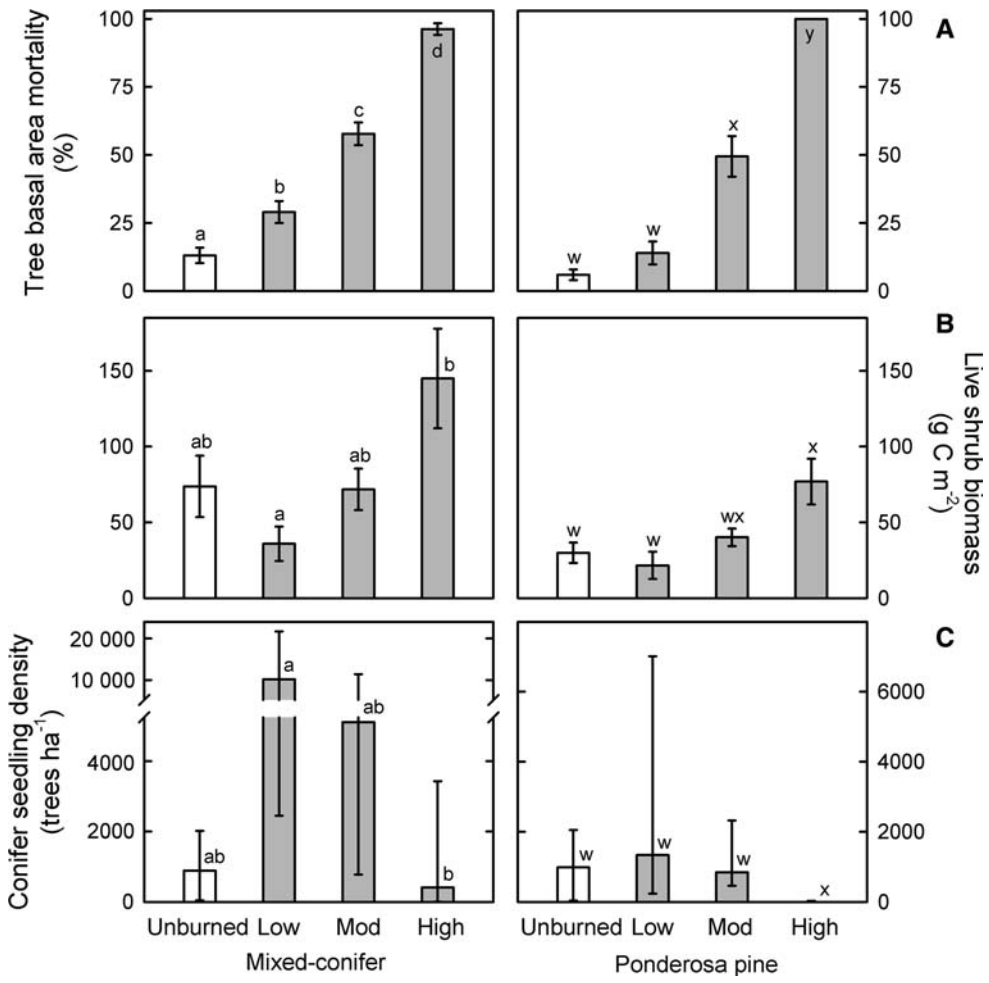

Figure 4. **A** Tree basal area (BA) mortality, **B** live shrub biomass, and **C** conifer seedling regeneration 4–5 years postfire by forest type and burn severity in the Metolius Watershed. Bars in **A** and **B** denote means; error bars denote ±1 SE from 8 plots in each forest type*burn severity treatment. Due to skewness, bars in **C** denote medians and error bars denote 25 and 75th percentile. Note the different scales between forest types above y-axis break in **C**. Tree mortality in **A** is % BA mortality due to fire in burned stands and total % dead BA in unburned stands. Lowercase letters denote statistically significant differences (Tukey-adjusted $P < 0.05$) among severities. Statistical tests for **A** used total % BA mortality, a metric common to all treatments. Statistical tests for **C** used $\log_e$-transformed data. **A** and **C** excluded the prefire biomass covariate. Seedlings are live, non-planted trees from the postfire time period only. Note that high-severity PP stands included 100% tree mortality in all 8 plots and a median seedling density of zero.

types (Table 4), although total ecosystem C was not significantly different among severities in MC forests ($P > 0.670$). In both types, fine root mass and soil C to 20 cm depth were not significantly different among severities ($P > 0.330$). Scaled to 100 cm, mean soil C stocks (±1 SE from regression) were 6556 ± 348 and 5903 ± 195 g C m^{-2} for burned MC and PP stands, respectively (Table 4). These values are similar to nearby unburned stands (7057 g C m^{-2}) and substantially lower than soil C in more mesic Oregon forests (14,244 and 36,174 g C m^{-2} in the West Cascades and Coast Range, respectively; Sun and others 2004). The lack of significant differences among severities furthers the evidence that soil C can be conserved with disturbance (Campbell and others 2009), including high-severity fire (Irvine and others 2007). Without site-specific prefire data we were unable to directly measure changes in soil C, and in applying a fixed-depth approach, a limitation of most postfire studies, we could not fully preclude the possibility of fire-induced soil C loss due to combustion, plume transport, or erosion (Bormann and others 2008). Unlike that study, in steep terrain experiencing stand-replacement fire (Bormann and others 2008), we did not observe severe erosion or changes in the soil surface between burned and unburned stands, and we detected no differences in

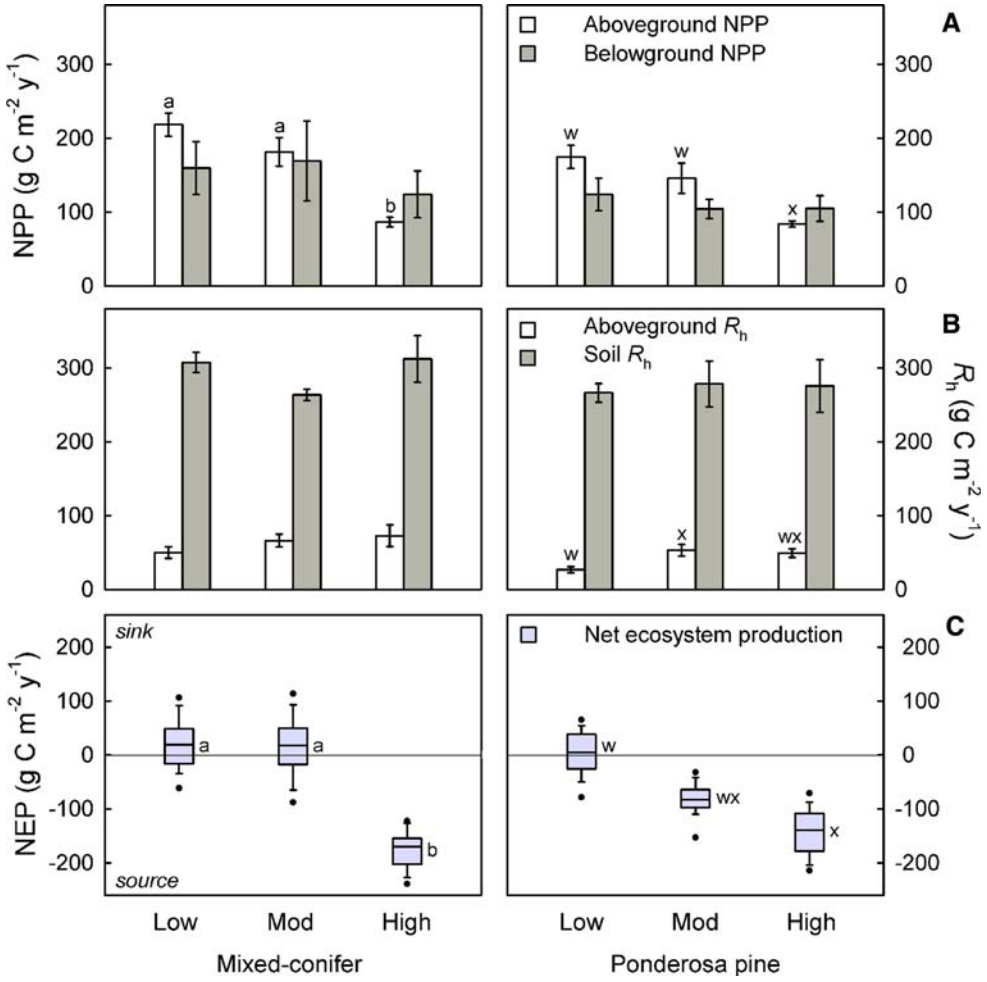

Figure 5. **A** Net primary productivity (NPP), **B** heterotrophic respiration (R_h), and **C** net ecosystem production (NEP) 4–5 years postfire by forest type and burn severity in the Metolius Watershed. Bars in **A** and **B** denote means; error bars denote ±1 SE from 8 plots in each forest type*burn severity treatment. Boxplots in **C** from Monte Carlo uncertainty propagation (see ''Methods''); line denotes median, box edges denote 25th and 75th percentiles, error bars denote 10th and 90th percentiles, and points denote 5th and 95th percentiles. Aboveground R_h includes all dead wood, shrubs, and herbaceous vegetation (Table 6). Soil R_h fractions from Irvine and others (2007). Lowercase letters denote statistically significant differences (Tukey-adjusted $P < 0.05$) among severities, tested with ANCOVA of each response variable given prefire biomass and burn severity.

mean or maximum soil depth among severities (Meigs 2009).

Our C pool estimates are consistent with previous estimates for PP in the Metolius area. Total aboveground C values for unburned and low-severity PP stands are similar to mature and young pine stands, respectively, whereas moderate- and high-severity stands fall between the values reported for initiation and young stands in a PP chronosequence (Law and others 2003). Our estimates of total ecosystem C in moderate- and high-severity PP stands are consistent with those reported by Irvine and others (2007). No analogous studies exist for the East Cascades MC forest type; the current study provides the first such estimates. The trends with burn severity were similar in both forest types, and the forest types differed consistently only in the magnitude of C pools. Total ecosystem C was 47% greater in MC forests than in PP forests (derived from Table 4).

Vegetation regeneration was generally robust but showed high variability and divergent responses of tree and non-tree functional types (Figure 4). Non-tree live biomass (that is, shrubs, forbs) was positively associated with burn severity, with significantly higher mass in high- versus low-severity stands ($P < 0.030$, Table 4, Figure 4). The strong shrub response—at or above prefire levels by 4–

5 years postfire—suggests important interactions with regenerating trees, which showed the opposite trend with burn severity. Tree seedling density (seedlings ha^{-1}) varied over 5 orders of magnitude (study wide range: 0–62,134) and, like shrub regeneration, was higher in MC than PP stands (Figure 4). This high variability is similar to studies of postfire conifer regeneration in the Klamath-Siskiyou and Rocky Mountain regions (5–6 orders of magnitude; Donato and others 2009b; Turner and others 2004), and the lack of PP regeneration in high-severity patches is consistent with previous studies reporting sparse regeneration beyond a generally short seed dispersal range (for example, Lentile and others 2005). Although regenerating vegetation represents a small C pool, it contributes to immediate postfire C uptake (described below) and sets the initial conditions for succession. The widespread presence of shrubs, particularly in high-severity stands, may initially reduce seedling growth through competition (Zavitkovski and Newton 1968), but over the long-term, understory shrubs play an important role in maintaining soil quality (C, N, microbial biomass C) in this ecoregion (Busse and others 1996). Because tree seedlings and shrubs were strongly correlated with overstory mortality, the burn severity mosaic could thus influence trajectories of C loss and accumulation for decades.

Postfire Carbon Balance (Biogenic C Fluxes and NEP)

Aboveground C Fluxes

Aboveground C fluxes followed the trends of live and dead C pools; NPP_A declined with increasing tree mortality (Figure 5A). In both forest types, NPP_A was significantly lower ($P < 0.015$) in high-severity versus moderate- and low-severity stands, which were not significantly different from each other ($P > 0.210$; overall range: 84–214 g C m^{-2} y^{-1}). Although NPP_A declined monotonically with burn severity, the sum of shrub and herbaceous NPP_A was about twofold higher in moderate- and high-severity versus low-severity stands, resulting in a dramatic increase in the non-tree proportion of NPP_A (Table 5). Thus, despite a reduction in live aboveground C of over 90% in both forest types in high-severity compared to low-severity stands, NPP_A was only 55% lower on average (Table 5). This trend, coupled with NPP_B (described below), resulted in a mean reduction of total NPP of about 40% from low- to high-severity, consistent with a strong compensatory effect of non-tree vegetation

Table 5. Annual Net Primary Productivity (NPP) of Burned Forest Stands in the Metolius Watershed

Forest type[1] / Burn severity	Aboveground				Belowground			Total NPP[7]	Non-tree[8] % of NPP_A	NPP_A:NPP_B ratio
	Tree[2]	Shrub	Herbaceous[3]	NPP_A[4]	Coarse root[2]	Fine root[5]	NPP_B[6]			
Mixed-conifer[1]	*93 (15)*	*20 (5)*	*46 (4)*	***159*** *(13)*	*18 (3)*	*132 (24)*	***150*** *(24)*	***309*** *(29)*	*42*	*1.06*
Low severity	$_{a}$173 (11)	8 (9)	33 (7)	$_{a}$**214** (15)	$_{a}$36 (3)	122 (44)	**159** (44)	**372** (47)	19	1.35
Mod severity	$_{b}$99 (11)	25 (9)	54 (7)	$_{a}$**178** (15)	$_{b}$18 (3)	151 (44)	**169** (43)	**347** (46)	44	1.05
High severity	$_{c}$12 (11)	27 (9)	51 (7)	$_{b}$**90** (15)	$_{c}$2 (3)	122 (44)	**125** (43)	**215** (46)	87	0.72
Ponderosa pine[1]	*68 (13)*	*10 (2)*	*57 (6)*	***135*** *(11)*	*10 (2)*	*96 (7)*	***107*** *(7)*	***242*** *(16)*	*50*	*1.26*
Low severity	$_{w}$135 (11)	3 (4)	$_{w}$34 (10)	$_{w}$**172** (15)	$_{w}$22 (2)	91 (13)	**113** (13)	$_{w}$**285** (24)	22	1.52
Mod severity	$_{x}$69 (12)	10 (4)	$_{x}$71 (10)	$_{w}$**151** (15)	$_{x}$9 (2)	101 (13)	**110** (13)	$_{wx}$**260** (24)	54	1.37
High severity	$_{y}$0 (0)	16 (4)	$_{wx}$68 (10)	$_{x}$**84** (15)	$_{y}$0 (0)	97 (13)	**97** (13)	$_{x}$**180** (24)	100	0.87

Notes: Values: mean NPP (g C m^{-2} y^{-1}). SE from ANCOVA in parentheses. Subscript letters indicate pairwise significant differences (Tukey-adjusted $P < 0.05$) between severities within each forest type. Summary fluxes bold.

[1] *Forest type row: italics denote values from burned stands only (n = 24; most NPP components not surveyed in unburned stands).*

[2] *Tree: sum of bole and foliage NPP_A. Coarse root NPP modeled from live tree DBH (6th column).*

[3] *Herbaceous: sum of graminoid and forb NPP_A, equal to dry mass.*

[4] *NPP_A: annual aboveground net primary productivity (bold, shown in Figure 4).*

[5] *Fine root NPP_B to 100 cm depth based on published turnover index (Andersen and others 2008) and total fine root mass scaled from 20 cm depth.*

[6] *NPP_B: annual belowground net primary productivity (bold, shown in Figure 4).*

[7] *Total NPP: sum of all above- and belowground fluxes entering the system (bold).*

[8] *Non-tree NPP_A: sum of shrub and herbaceous NPP_A.*

NPP_A. Previous studies in clearcut, thinned, and burned forests have shown the same pattern of rapid recolonization by non-trees contributing disproportionately to NPP (Campbell and others 2004; Gough and others 2007; Irvine and others 2007; Campbell and others 2009), and this study furthers the evidence across the severity gradient in two forest types. These findings suggest that fire studies focused solely on tree C pools (for example, Hurteau and others 2008) result in systematic biases and that C models and policies (for example, CCAR 2007) should encompass the full suite of ecosystem components and processes, including multiple vegetation functional types and rapid belowground recovery following disturbance.

Heterotrophic respiration of aboveground necromass (R_{hWD}), computed from C pools and decomposition constants, was a substantial component of C balance across both forest types but showed weak trends among severities (Figure 5B, Table 6). Despite the increase in dead wood mass with severity (Table 4), there were no significant differences in MC stands and only suggestive increases of R_{hWD} with severity in PP stands ($P = 0.031$–0.051). We attribute this surprising result to several factors: differing species- and decay class-specific constants and high variability among plots and severities; high retention and slow decomposition of snags; relatively high snag and dead shrub R_{hWD} in low-severity MC stands; relatively low CWD and dead shrub R_{hWD} in high-severity PP stands (Table 6). Although we expected that the immediate postfire period would exhibit maximum necromass over successional time (Wirth and others 2002; Hicke and others 2003), our R_{hWD} estimates were well less than both NPP_A and NPP_B ($R_{hWD} < 35\%$ of total NPP). In addition, R_{hWD} 4–5 years postfire constituted about 15% of total R_h across both forest types; R_{hsoil} (described below) accounted for approximately 85% (Table 6), demonstrating that belowground respiration processes are the predominant drivers of C loss.

Our range of R_{hWD} across the two forest types (28–75 g C m^{-2} y^{-1}; Table 6) is higher than estimates 2 years postfire in PP forest (Irvine and others 2007), similar to young PP stands in the Metolius area (Sun and others 2004) and an old-growth *Pseudotsuga-Tsuga* forest about 100 km away (Harmon and others 2004), and much less than untreated and thinned PP stands in Northern California (Campbell and others 2009). Our relatively low R_{hWD} estimates, particularly compared to C assimilation (NPP), illustrate the importance of decomposition lags in seasonally arid ecosystems, where microbial snag decomposition is moisture-limited. Other systems, such as sub-tropical humid zones where decomposition is not moisture- or temperature-limited and disturbance rapidly generates downed woody detritus (for example, hurricanes; Chambers and others 2007), may experience a more rapid pulse of C emission from necromass. The notion that fire-killed necromass represents a large, rapid C loss is unfounded, however, and warrants further investigation.

Woody detritus decomposition is a highly uncertain process, particularly in burned forests, where charring and snag fall play important, contrasting roles. For these R_{hWD} estimates, we used available decomposition constants derived from unburned forests. We believe that charring would likely reduce decomposition rates (DeLuca and Aplet 2008; Donato and others 2009a) but tested the sensitivity of our estimates by assuming snag decay rates equivalent to CWD. In this scenario, mean R_{hWD} would be approximately 125% and 50% higher in MC and PP stands, respectively, pushing low-severity stands into a net C source (negative NEP, although mean R_{hWD} would remain $<50\%$ of R_{hsoil} in both forest types). Our use of the 10% fraction is consistent with previous studies (Irvine and others 2007), and other studies have assumed zero snag decomposition (for example, Wirth and others 2002). Our short-term study precluded the assessment of snag fall, a stochastic process dependent on many factors (Russell and others 2006). The fall rates reported by Russell and others (2006)—snag half-lives for ponderosa pine and Douglas fir of 9–10 and 15–16 years, respectively—suggest that the majority of snags generated in the Metolius fires will stay standing for at least 10 years postfire. R_{hWD} may increase with accelerating snag fall (particularly in high-severity stands) but will remain small relative to R_{hsoil}, and NPP will likely increase over the same time period. Future studies are necessary to reduce the uncertainty of decomposition and snag dynamics in this area.

Belowground C Fluxes

Belowground C fluxes were by far the largest and most variable components of the annual C budget (NEP; Figure 5). Belowground NPP (NPP_B) was not significantly different across the entire study (overall mean: 284 g C m^{-2} y^{-1}; $P > 0.680$ in both forest types). Fine root NPP_B to 100 cm, based on total fine root mass and a constant turnover rate, accounted for about 90% of NPP_B, with increasing importance in high-severity stands, where very few live tree coarse roots survived. The apparent rapid establishment of fine roots in high-severity stands

Table 6. Annual Heterotrophic Respiration (R_h) and NEP of Forest Stands in the Metolius Watershed

Forest type[1] Burn severity	Aboveground (R_{hWD})						Belowground		Total R_h[7]	NEP[8]	NPP:R_h ratio[8]
	Snag[2]	Stump[2]	CWD[3]	Dead shrub	Herbaceous[4]	R_{hWD}[5]	R_{hsoil}[6]	R_{hsoil}:R_{soil} ratio[6]			
Mixed-conifer[1]	7 (1)	5 (1)	24 (4)	3 (2)	22 (2)	**61** (6)	*294* (*12*)	*na*	***357*** (*12*)	*−44* (*28*)	*0.87*
Unburned	3 (2)	7 (1)	29 (9)	1 (4)	19 (4)	**59** (12)	na (na)	na	**na** (na)	na (na)	na
Low severity	7 (2)	3 (1)	14 (9)	7 (4)	17 (4)	**47** (12)	305 (21)	0.48	**353** (20)	$_{a}$21 (48)	1.05
Mod severity	9 (2)	5 (1)	22 (9)	1 (4)	27 (4)	**64** (12)	261 (21)	0.52	**327** (19)	$_{a}$21 (55)	1.06
High severity	9 (2)	5 (1)	32 (9)	3 (4)	26 (4)	**75** (12)	314 (21)	0.56	**388** (19)	$_{b}$-174 (32)	0.55
Ponderosa pine[1]	2 (1)	3 (1)	9 (2)	2 (1)	26 (3)	**42** (3)	*274* (*15*)	*na*	***317*** (*17*)	*−76* (*20*)	*0.76*
Unburned	$_{w}$0 (1)	4 (1)	$_{w}$18 (3)	2 (2)	$_{w}$16 (4)	**$_{wx}$39** (6)	na (na)	na	**na** (na)	na (na)	na
Low severity	$_{wx}$1 (1)	3 (1)	$_{x}$5 (3)	2 (2)	$_{w}$17 (4)	**$_{w}$27** (6)	262 (28)	0.48	**290** (30)	$_{w}$0 (33)	0.98
Mod severity	$_{wx}$2 (1)	3 (1)	$_{wx}$8 (3)	4 (2)	$_{x}$36 (4)	**$_{x}$53** (6)	286 (28)	0.52	**338** (31)	$_{wx}$-87 (35)	0.77
High severity	$_{x}$5 (1)	3 (1)	$_{wx}$7 (3)	1 (2)	$_{x}$34 (4)	**$_{wx}$49** (6)	274 (28)	0.56	**324** (30)	$_{x}$-142 (37)	0.56

Notes: Values: mean R_h (g C m^{-2} y^{-1}). SE from ANCOVA in parentheses, except NEP SE from Monte Carlo. Subscript letters Indicate pairwise significant differences (Tukey-adjusted $P < 0.05$) between severities within each forest type. Summary fluxes bold.

[1]Forest type row: non-italics denote all stands (unburned and burned, n = 32); italics denote burned stands only (n = 24, unburned stands not surveyed [na]).

[2]Snag R_h uses 10% of CWD decay rate and stump R_h uses 100% of CWD decay rate.

[3]CWD R_h includes FWD R_h, which was less than 0.15% of CWD R_h in all treatments.

[4]Herbaceous: forb and graminoid combined (assumed 50% of dry mass).

[5]R_{hWD}: sum of aboveground components (bold). Includes herbaceous annual decomposition (50% of dry mass).

[6]R_{hsoil}: heterotrophic soil respiration, based on total soil efflux and heterotrophic fractions from Irvine and others (2007). Moderate severity fraction is mean of unburned and high severity fractions.

[7]Total R_h: sum of all above- and belowground fluxes from land to atmosphere (bold).

[8]Net ecosystem production: sum of NPP (Table 5) and R_h fluxes. SE from Monte Carlo uncertainty propagation. NPP:R_h ratio < 1 if negative NEP.

contributed to the strong NPP compensatory effect of non-tree vegetation (Table 5). NPP_B accounted for approximately 50% of total NPP averaged across all severities and forest types, but high-severity stands in both forest types exhibited higher NPP_B than NPP_A (NPP_B = 58 and 54% of total NPP in MC and PP, respectively), indicating belowground C allocation values between those reported for grasslands and shrublands (67 and 50%, respectively; Chapin and others 2002). These estimates of fine root NPP_B are very similar to those reported for moderate- and high-severity PP by Irvine and others (2007), even though that study accounted for fire-induced fine root mortality and computed fine root NPP from live rather than total fine root stocks. Our estimated FR NPP is higher than a thinned PP forest in Northern California (Campbell and others 2009) and lower than a mixed-deciduous forest in Michigan (Gough and others 2007). Our estimates of total NPP (approximately 200–400 g C m^{-2} y^{-1}) and NPP_A:NPP_B ratio (overall mean: 1.15; Table 5) are within the range of previous studies in the area (Law and others 2003; Campbell and others 2004) and consistent with the postfire C allocation patterns described by Irvine and others (2007).

Heterotrophic soil respiration (R_{hsoil}) was not significantly different among burn severities and forest types ($P > 0.200$; Figure 5B, Table 6), consistent with the trends of forest floor, fine roots, and soil C (Table 4). Mean annual R_{hsoil} (g C m^{-2} y^{-1}, ±1 SE from regression) was 294 ± 12 and 274 ± 15 in MC and PP stands, respectively, very similar to previous estimates in mature unburned PP stands (Law and others 2003; Sun and others 2004). The lack of R_{hsoil} differences among severity classes and similarity to unburned forest suggests that this flux is resistant to disturbance-induced changes in these forests and supports the findings of previous studies (Irvine and others 2007; Campbell and others 2009). R_{hsoil} chamber measurements 1 year postfire in a nearby high-severity PP site on the 2006 Black Crater fire (J. Martin, unpublished data) were similar to unburned PP forest (Irvine and others 2008) and the values in the current study, indicating the lack of a large R_{hsoil} pulse from 1–5 years postfire. Although we did not find evidence of this postfire pulse in the absolute magnitude of R_{hsoil}, the conservation of R_{hsoil} across severities, coupled with declines in NPP, resulted in a large decline of the NPP:R_h ratio (approximately 0.55 in high-severity stands, both forest types; Table 6). This increase in relative R_{hsoil} equated to a muted postfire pulse that is reflected in our NEP estimates.

Implications for NEP

In both forest types, NPP_A was the principal driver of NEP trends, whereas R_{hsoil} controlled NEP magnitudes (Figure 5, Table 6). NEP was significantly lower in high- versus low-severity stands in both forest types ($P < 0.035$). In MC stands, mean NEP (g C m^{-2} y^{-1}, ± 1 SE from Monte Carlo simulations) varied from a slight sink (21 ± 48 and 21 ± 55) in low- and moderate-severity stands to a substantial source in high-severity stands (−174 ± 32). In PP forest, mean NEP declined from C neutral in low-severity stands (0 ± 33) to an intermediate source in moderate-severity stands (−87 ± 35) and substantial source in high-severity stands (−142 ± 37). Thus, mean annual NEP was similar in high-severity stands of both forest types 4–5 years after fire. These results are consistent with previous estimates of NPP, R_h, and NEP in unburned, moderate-, and high-severity PP stands within the study area (Irvine and others 2007), although our NEP estimate for high-severity stands is lower.

Previous studies quantified a NEP recovery period to a net sink of 20–30 years in PP forest following stand-replacement clearcutting (Law and others 2003; Campbell and others 2004). Longer-term measurements are necessary to determine the NEP fate of these postfire stands, but less than 30 years seems appropriate for high-severity stands, which are already closer to zero than initiation stands described by Law and others (2003), despite the removal of necromass via timber harvest in that study and higher R_{hWD} estimates here. In both forest types, low-severity NEP was not significantly different from zero (error estimates include zero; Table 6, Figure 5), which may be explained by limited fire effects and/or relatively rapid recovery of NEP. Although not a large C source to the atmosphere, C neutral stands represent a substantial decline from prefire NEP (unburned PP mean ± 1 SE for a range of age classes: 50 ± 14 g C m^{-2} y^{-1}, Irvine and others 2007). Management actions that mimic low-severity fire via prescribed burning or thinning (thus removing C) will likely reduce short-term NEP and long-term average C storage (Campbell and others 2009; Mitchell and others 2009), although strategic fuels treatments may help stabilize large tree C pools (North and others 2009).

Conclusion

The 2002–2003 wildfires across the Metolius Watershed generated a heterogeneous landscape pattern of overstory tree mortality and associated transformations of C pools and fluxes. Our results

provide new constraints on short-term fire effects (4–5 years postfire) for regional C policy frameworks and underscore the importance of accounting for the full gradient of forest disturbance processes. Specifically, we found:

1. Stand-scale C combustion varied with burn severity from 13 to 35% of prefire aboveground C pools, with the largest emission proportion from combustion of surface/ground fuels and a study-wide average live tree stem consumption of 1.24%. Landscape-scale pyrogenic C emissions were equivalent to 2.5% of Oregon statewide anthropogenic CO_2 emissions from fossil fuel combustion and industrial processes for the same 2-year period.
2. Overstory live tree mass and seedling density decreased with increasing burn severity, whereas live shrub and herbaceous mass showed the opposite trend. From low- to moderate- to high-severity stands, average tree basal area mortality was 14, 49, and 100% in ponderosa pine, and 29, 58, and 96% in mixed-conifer forests.
3. Despite this decline in live aboveground C pools, total net primary productivity was only 40% lower in high- versus low-severity stands, reflecting a strong compensatory effect of nontree productivity. Thus, the rapid response of early successional vegetation offset declines in NPP and NEP, buffering potential fire impacts on stand and landscape C storage, particularly when combined with the protracted decomposition of dead mass and conservation of belowground components (soil C, R_{hsoil}, and NPP_B).

With predictions of accelerating climate change and increasing fire extent and severity in western North American forests (IPCC 2007; Balshi and others 2009; Miller and others 2009), long-term field measurements are essential to assess trends in C storage and net annual C uptake over the course of several fire cycles, as well as any potential for directional ecosystem responses over time (for example, state change). Because non-stand-replacement fire accounts for the majority of the annual burned area in the Pacific Northwest Region (Schwind 2008), studies that focus exclusively on high-severity patches systematically underestimate pyrogenic C emission, mortality, and reduced C uptake following fire, impacts that will likely play an increasingly important role in regional and global carbon cycling.

ACKNOWLEDGMENTS

This research was supported by the Office of Science (BER), U.S. Department of Energy, Grant No. DE-FG02-06ER64318 and the College of Forestry, Oregon State University. We thank A. Pfleeger, P. Bozarth-Dreher, L. Gupta, R. Gupta, C. Sodemann, and C. Hebel for field and lab assistance. We acknowledge the insightful reviews of W. Cohen, C. Dunn, F. Gonçalves, C. Hebel, P. Hessburg, J. Meigs, D. Turner, and two anonymous reviewers. M. Huso provided invaluable statistical assistance, and the OSU Central Analytical Laboratory performed thorough, efficient chemical analysis. M. Duane, K. Howell, T. Hudiburg, J. Irvine, R. Kennedy, R. Ottmar, S. Powell, S. Prichard, C. Sierra, C. Thomas, H. Zald, and the OSU Pyro-maniacs assisted with data analysis. G. Fiske and K. Olsen helped with Figure 1 cartography. We thank the Deschutes National Forest for GIS data and access to field sites.

REFERENCES

Amiro BD, Todd JB, Wotton BM, Logan KA, Flannigan MD, Stocks BJ, Mason JA, Martell DL, Hirsch KG. 2001. Direct carbon emissions from Canadian forest fires, 1959–1999. Can J For Res 31:512–25.

Andersen CP, Phillips DL, Rygiewicz PT, Storm MJ. 2008. Fine root growth and mortality in different-aged ponderosa pine stands. Can J For Res 38:1797–806.

Balshi MS, McGuire AD, Duffy P, Flannigan M, Walsh J, Melillo JM. 2009. Assessing the response of area burned to changing climate in western boreal North America using a Multivariate Adaptive Regression Splines (MARS) approach. Glob Change Biol 15:578–600.

Birdsey RA, Jenkins JC, Johnston M, Huber-Sannwald E, Amiro BD, de Jong B, Barra JDE, French NHF, Garcia-Oliva F, Harmon ME, Heath LS, Jaramillo VJ, Johnsen K, Law BE, Marín-Spiotta E, Masera O, Neilson R, Pan Y, Pregitzer KS. 2007. North American forests. In: King AW, Dilling L, Zimmerman GP, Fairman DM, Houghton RA, Marland G, Rose AZ, Wilbanks TJ, Eds. The first State of the Carbon Cycle Report (SOCCR): The North American carbon budget and implications for the global carbon cycle. A report by the U.S. Climate Change Science Program and the Subcommittee on Global Change Research. Asheville: National Oceanic and Atmospheric Administration National Climatic Data Center. p 117–26.

Bork BJ. 1985. Fire history in three vegetation types on the eastern side of the Oregon Cascades. PhD Thesis, Oregon State University. 94 p.

Bormann BT, Homann PS, Darbyshire RL, Morrissette BA. 2008. Intense forest wildfire sharply reduces mineral soil C and N: the first direct evidence. Can J For Res 38:2771–83.

Brown JK. 1974. Handbook for inventorying downed woods material. USDA Forest Service General Technical Report INT-GTR-16. Ogden.

Busse MD, Cochran PH, Barren JW. 1996. Changes in ponderosa pine site productivity following removal of understory vegetation. Soil Sci Soc Am J 60:1614–21.

Campbell JL, Alberti G, Martin JG, Law BE. 2009. Carbon dynamics of a ponderosa pine plantation following a thinning treatment in the northern Sierra Nevada. For Ecol Manag 257:453–63.

Campbell JL, Donato DC, Azuma DL, Law BE. 2007. Pyrogenic carbon emission from a large wildfire in Oregon, United States. J Geophys Res 112:G04014.

Campbell JL, Law BE. 2005. Forest soil respiration across three climatically distinct chronosequences in Oregon. Biogeochemistry 73:109–25.

Campbell JL, Sun OJ, Law BE. 2004. Disturbance and net ecosystem production across three climatically distinct forest landscapes. Glob Biogeochem Cycles 18.

CCAR. 2007. Forest sector protocol version 2.1. California Climate Action Registry (CCAR). http://www.climateregistry.org/tools/protocols/industry-specific-protocols.html.

Chambers JQ, Fisher JI, Zeng HC, Chapman EL, Baker DB, Hurtt GC. 2007. Hurricane Katrina's carbon footprint on U. S. Gulf Coast forests. Science 318:1107.

Chapin FSIII, Matson PA, Mooney HA. 2002. Principles of terrestrial ecosystem ecology. New York: Springer.

Chapin FSIII, Woodwell GM, Randerson JT, Rastetter EB, Lovett GM, Baldocchi DD, Clark DA, Harmon ME, Schimel DS, Valentini R, Wirth C, Aber JD, Cole JJ, Goulden ML, Harden JW, Heimann M, Howarth RW, Matson PA, McGuire AD, Melillo JM, Mooney HA, Neff JC, Houghton RA, Pace ML, Ryan MG, Running SW, Sala OE, Schlesinger WH, Schulze ED. 2006. Reconciling carbon-cycle concepts, terminology, and methods. Ecosystems 9:1041–50.

Chen H, Harmon ME, Sexton JM, Fasth B. 2002. Fine-root decomposition and N dynamics in coniferous forests of the Pacific Northwest, USA. Can J For Res 32:320–31.

Cline SP, Berg AB, Wight HM. 1980. Snag characteristics and dynamics in Douglas-fir forests, western Oregon. J Wildlife Manag 44:773–86.

Daly C, Gibson WP, Taylor GH, Johnson GL, Pasteris P. 2002. A knowledge-based approach to the statistical mapping of climate. Clim Res 22:99–113.

DAYMET. 2009. Distributed climate data, http://www.daymet.org/.

DeLuca TH, Aplet GH. 2008. Charcoal and carbon storage in forest soils of the Rocky Mountain West. Front Ecol Environ 6:18–24.

Donato DC, Campbell JL, Fontaine JB, Law BE. 2009a. Quantifying char in postfire woody detritus inventories. Fire Ecol 5(2):104–115.

Donato DC, Fontaine JB, Campbell JL, Robinson WD, Kauffman JB, Law BE. 2009b. Early conifer regeneration in stand-replacement portions of a large mixed-severity wildfire in the Siskiyou Mountains, Oregon. Can J For Res 39:823–38.

Dore S, Kolb TE, Montes-Helu M, Sullivan BW, Winslow WD, Hart SC, Kaye JP, Koch GW, Hungate BA. 2008. Long-term impact of a stand-replacing fire on ecosystem CO_2 exchange of a ponderosa pine forest. Glob Change Biol 14:1801–20.

Eyre FH, Eds.1980. Forest cover types of the United States and Canada. Society of American Foresters, Washington, DC.

Fitzgerald SA. 2005. Fire ecology of ponderosa pine and the rebuilding of fire-resilient ponderosa pine ecosystems. In: Proceedings of the symposium on ponderosa pine: issues, trends, and management. USDA Forest Service General Technical Report PSW-GTR-198, 18–21 October 2004, Klamath Falls, OR, Albany.

Franklin JF, Dyrness CT. 1973. Natural vegetation of Oregon and Washington. USDA Forest Service General Technical Report PNW-GTR-8. Portland.

Franklin SE, Waring RH, McCreight RW, Cohen WB, Fiorella M. 1995. Aerial and satellite sensor detection and classification of western spruce budworm defoliation in a subalpine forest. Can J Remote Sens 21:299–308.

French NHF, Kasischke ES, Hall RJ, Murphy KA, Verbyla DL, Hoy EE, Allen JL. 2008. Using Landsat data to assess fire and burn severity in the North American boreal forest region: an overview and summary of results. Int J Wildland Fire 17:443–62.

Goward SN, Masek JG, Cohen WB, Moisen G, Collatz GJ, Healey SP, Houghton RA, Huang C, Kennedy RE, Law BE, Powell SL, Turner DP, Wulder MA. 2008. Forest disturbance and North American carbon flux Eos, transactions. Am Geophys Union 89:105–16.

Gough CM, Vogel CS, Harrold KH, George K, Curtis PS. 2007. The legacy of harvest and fire on ecosystem carbon storage in a north temperate forest. Glob Change Biol 13:1935–49.

Harmon ME, Bible K, Ryan MG, Shaw DC, Chen H, Klopatek J, Li X. 2004. Production, respiration, and overall carbon balance in an old-growth *Pseudotsuga-tsuga* forest ecosystem. Ecosystems 7:498–512.

Harmon ME, Fasth B, Sexton JM. 2005. Bole decomposition rates of seventeen tree species in Western U.S.A.: a report prepared for the Pacific Northwest Experiment Station, the Joint Fire Sciences Program, and the Forest Management Service Center of WO Forest Management Staff. http://andrewsforest.oregonstate.edu/pubs/webdocs/reports/decomp/cwd_decomp_web.htm.

Harmon ME, Sexton JM. 1996. Guidelines for measurements of woody detritus in forest ecosystems. U.S. long term ecological research program network, vol. 20. Albuquerque.

Hessburg PF, Salter RB, James KM. 2007. Re-examining fire severity relations in pre-management era mixed conifer forests: inferences from landscape patterns of forest structure. Landsc Ecol 22:5–24.

Hicke JA, Asner GP, Kasischke ES, French NHF, Randerson JT, Collatz GJ, Stocks BJ, Tucker CJ, Los SO, Field CB. 2003. Postfire response of North American boreal forest net primary productivity analyzed with satellite observations. Glob Change Biol 9:1145–57.

Hudiburg T. 2008. Climate, management, and forest type influences on carbon dynamics of West-Coast US forests. M.S. Thesis, Oregon State University. 86 p.

Hudiburg T, Law BE, Turner DP, Campbell JL, Donato DC, Duane M. 2009. Carbon dynamics of Oregon and Northern California forests and potential land-based carbon storage. Ecol Appl 19:163–80.

Hurteau MD, Koch GW, Hungate BA. 2008. Carbon protection and fire risk reduction: toward a full accounting of forest carbon offsets. Front Ecol Environ 6:493–8.

IPCC. 2007. Climate change 2007: the physical science basis. In: Solomon S, Qin D, Manning M, Chen Z, Marquis M, Averyt KB, Tignor M, Miller HL, Eds. Contribution of working group I to the fourth assessment report of the intergovernmental panel on climate change (IPCC). Cambridge University Press, Cambridge, United Kingdom and New York. http://www.ipcc.ch.

Irvine J, Law BE, Hibbard KA. 2007. Postfire carbon pools and fluxes in semiarid ponderosa pine in Central Oregon. Glob Change Biol 13:1748–60.

Irvine J, Law BE, Martin JG, Vickers D. 2008. Interannual variation in soil CO_2 efflux and the response of root respiration to climate and canopy gas exchange in mature ponderosa pine. Glob Change Biol 14:2848–59.

Kashian DM, Romme WH, Tinker DB, Turner MG, Ryan MG. 2006. Carbon storage on landscapes with stand-replacing fires. Bioscience 56:598–606.

Keane RE, Agee JK, Fulé P, Keeley JE, Key C, Kitchen SG, Miller R, Schulte LA. 2008. Ecological effects of large fires on US landscapes: benefit or catastrophe? Int J Wildland Fire 17:696–712.

Key CH, Benson NC. 2006. Landscape assessment: Ground measure of severity, the Composite Burn Index; and remote sensing of severity, the Normalized Burn Ratio. In Lutes DC, et al, Eds. FIREMON: Fire effects monitoring and inventory system. USDA Forest Service General Technical Report RMRS-GTR-164-CD. Fort Collins.

Kurz WA, Stinson G, Rampley GJ, Dymond CC, Neilson ET. 2008. Risk of natural disturbances makes future contribution of Canada's forests to the global carbon cycle highly uncertain. Proc Natl Acad Sci USA 105:1551–5.

Law BE, Arkebauer T, Campbell JL, Chen J, Sun O, Schwartz M, van Ingen C, Verma S. 2008. Terrestrial carbon observations: Protocols for vegetation sampling and data submission. Report 55, Global Terrestrial Observing System. FAO, Rome. 87 pp.

Law BE, Ryan MG, Anthoni PM. 1999. Seasonal and annual respiration of a ponderosa pine ecosystem. Glob Change Biol 5:169–82.

Law BE, Sun OJ, Campbell JL, Van Tuyl S, Thornton PE. 2003. Changes in carbon storage and fluxes in a chronosequence of ponderosa pine. Glob Change Biol 9:510–24.

Law BE, Thornton PE, Irvine J, Anthoni PM, Van Tuyl S. 2001a. Carbon storage and fluxes in ponderosa pine forests at different developmental stages. Glob Change Biol 7:755–77.

Law BE, Van Tuyl S, Cescatti A, Baldocchi DD. 2001b. Estimation of leaf area index in open-canopy ponderosa pine forests at different successional stages and management regimes in Oregon. Agric For Meteorol 108:1–14.

Law BE, Waring RH. 1994. Combining remote sensing and climatic data to estimate net primary production across Oregon. Ecol Appl 4:717–28.

Lentile LB, Smith FW, Shepperd WD. 2005. Patch structure, fire-scar formation, and tree regeneration in a large mixed-severity fire in the South Dakota Black Hills, USA. Can J For Res 35:2875–85.

Martin RE, Sapsis DB. 1991. Fires as agents of biodiversity: pyrodiversity promotes biodiversity. In: Harris RR, Erman DE, Kerner HM (technical coordinators), Eds. Proceedings of the symposium on biodiversity of northwestern California. Santa Rosa, CA: Wildland Resources Center, pp. 150–7.

Maser C, Anderson RG, Cromack Jr K, Williams JT, Martin RE. 1979. Dead and down woody material. Wildlife habitats in managed forests of the Blue Mountains of Oregon and Washington, USDA Forest Service Agriculture Handbook No. 553.

McIver JD, Ottmar RD. 2007. Fuel mass and stand structure after post-fire logging of a severely burned ponderosa pine forest in northeastern Oregon. For Ecol Manag 238:268–79.

Meigs GW. 2009. Carbon dynamics following landscape fire: influence of burn severity, climate, and stand history in the Metolius Watershed, Oregon. M.S. Thesis, Oregon State University. 147 p.

Miller JD, Safford HD, Crimmins M, Thode AE. 2009. Quantitative evidence for increasing forest fire severity in the Sierra Nevada and Southern Cascade Mountains, California and Nevada, USA. Ecosystems 12:16–32.

Mitchell SR, Harmon ME, O'Connell KEB. 2009. Forest fuel reduction alters fire severity and long-term carbon storage in three Pacific Northwest ecosystems. Ecol Appl 19:643–55.

Monsanto PG, Agee JK. 2008. Long-term post-wildfire dynamics of coarse woody debris after salvage logging and implications for soil heating in dry forests of the eastern Cascades, Washington. For Ecol Manag 255:3952–61.

North M, Hurteau M, Innes J. 2009. Fire suppression and fuels treatment effects on mixed-conifer carbon stocks and emissions. Ecol Appl 19:1385–96.

Ottmar RD, Sandberg DV, Riccardi CL, Prichard SJ. 2007. An overview of the fuel characteristic classification system—quantifying, classifying, and creating fuelbeds for resource planning. Can J For Res 37:2383–93.

Pierce LL, Running SW. 1988. Rapid estimation of coniferous forest leaf-area index using a portable integrating radiometer. Ecology 69:1762–7.

Prichard SJ, Ottmar RD, Anderson GK. 2006. Consume 3.0 user's guide. Pacific Wildland Fire Sciences Laboratory, USDA Forest Service, Pacific Northwest Research Station. Seattle, WA. http://www.fs.fed.us/pnw/fera/research/smoke/consume/index.shtml.

Rorig ML, Ferguson SA. 1999. Characteristics of lightning and wildland fire ignition in the Pacific Northwest. J Appl Meteorol 38:1565–75.

Roy DR, Boschetti L, Trigg SN. 2006. Remote sensing of fire severity: assessing the performance of the normalized burn ratio. IEEE Geosci Remote Sens Lett 3:112–6.

Running SW. 2008. Ecosystem disturbance, carbon, and climate. Science 321:652–3.

Russell RE, Saab VA, Dudley JG, Rotella JJ. 2006. Snag longevity in relation to wildfire and postfire salvage logging. For Ecol Manag 232:179–87.

Santantonio D, Hermann RK, Overton WS. 1977. Root biomass studies in forest ecosystems. Pedobiologia 17:1–31.

Savage M, Mast JN. 2005. How resilient are southwestern ponderosa pine forests after crown fires? Can J For Res 35:967–77.

Schoennagel T, Veblen TT, Romme WH. 2004. The interaction of fire, fuels, and climate across Rocky Mountain forests. Bioscience 54:661–76.

Schwind B. 2008. Monitoring trends in burn severity: report on the Pacific Northwest and Pacific Southwest fires—1984 to 2005. Available online: http://mtbs.gov.

Simon SA. 1991. Fire history in the Jefferson Wilderness area of east of the Cascade Crest. A final report to the Deschutes National Forest Fire Staff.

Soeriaatmadhe RE. 1966. Fire history of the ponderosa pine forests of the Warm Springs Indian Reservation Oregon. PhD Thesis, Oregon State University.

Sun OJ, Campbell JL, Law BE, Wolf V. 2004. Dynamics of carbon stocks in soils and detritus across chronosequences of different forest types in the Pacific Northwest, USA. Glob Change Biol 10:1470–81.

Swedberg KC. 1973. A transition coniferous forest in the Cascade Mountains of Northern Oregon. Am Midl Nat 89:1–25.

Thomas CK, Law BE, Irvine J, Martin JG, Pettijohn JC, Davis KJ. 2009. Seasonal hydrology explains inter-annual and seasonal variation in carbon and water exchange in a semi-arid mature ponderosa pine forest in Central Oregon. J Geophys Res Biogeosci. doi:10.1029/2009JG001010.

Thompson JR, Spies TA, Ganio LM. 2007. Reburn severity in managed and unmanaged vegetation in a large wildfire. Proc Natl Acad Sci USA 104:10743–8.

Thornton PE, Running SW, White MA. 1997. Generating surfaces of daily meteorological variables over large regions of complex terrain. J Hydrol 190:214–51.

Turner DP, Ritts WD, Law BE, Cohen WB, Yang Z, Hudiburg T, Campbell JL, Duane M. 2007. Scaling net ecosystem production and net biome production over a heterogeneous region in the western United States. Biogeosciences 4:597–612.

Turner MG, Tinker DB, Romme WH, Kashian DM, Litton CM. 2004. Landscape patterns of sapling density, leaf area, and aboveground net primary production in postfire lodgepole pine forests, Yellowstone National Park (USA). Ecosystems 7:751–75.

USDA. 2003. Field instructions for the annual inventory of Washington, Oregon, and California Forest Inventory and Analysis Program. USDA Forest Service Pacific Northwest Research Station. Portland.

Van Tuyl S, Law BE, Turner DP, Gitelman AI. 2005. Variability in net primary production and carbon storage in biomass across Oregon forests: an assessment integrating data from forest inventories, intensive sites, and remote sensing. For Ecol Manag 209:273–91.

Van Wagner CE. 1968. The line intersect method in forest fuel sampling. For Sci 14:20–6.

Weaver H. 1959. Ecological changes in the ponderosa pine forest of the Warm Springs Indian Reservation in Oregon. J For 57:15–20.

Westerling AL, Hidalgo HG, Cayan DR, Swetnam TW. 2006. Warming and earlier spring increase western US forest wildfire activity. Science 313:940–3.

Wirth C, Czimczik CI, Schulze ED. 2002. Beyond annual budgets: carbon flux at different temporal scales in fire-prone Siberian Scots pine forests. Tellus B Chem Phys Meteorol 54:611–30.

Zavitkovski J, Newton M. 1968. Ecological importance of snowbrush *Ceanothus velutinus* in the Oregon Cascades. Ecology 49:1134–45.